Organic & Biomolecular Chemistry

Accepted Manuscript

This article can be cited before page numbers have been issued, to do this please use: R. Zagami, C. Gangemi, G. Nocito, A. Aricò, M. Monforte, P. M. Bonaccorsi and A. Mazzaglia, *Org. Biomol. Chem.*, 2026, DOI: 10.1039/D6OB00537C.

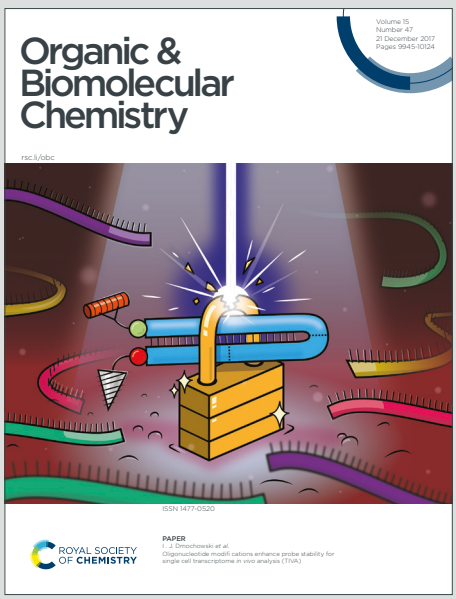

ROYAL SOCIETY OF CHEMISTRY

rsc.li/obc

View Article Online
DOI: 10.1039/D6OB00537C

ARTICLE

A supramolecular assembly of a disulfide linked adamantane-curcumin conjugate with amphiphilic cyclodextrin with redox-responsive potential

Received 00th January 20xx,
Accepted 00th January 20xx

DOI: 10.1039/x0xx00000x

Roberto Zagami,[a,b] Chiara M. A. Gangemi,[*a] Giuseppe Nocito,[b] Alberto Aricò,[a] Maura Monforte,[a] Paola M. Bonaccorsi[a] and Antonino Mazzaglia[*b]

The synthesis of a novel unsymmetrical disulfide linked adamantane-curcumin conjugate and its supramolecular assembly with amphiphilic cyclodextrin in aqueos dispersion is here reported. Within the nanoassemblies, curcumin derivative was dissolved up to 0.14 mg/mL in ultrapure water and showed high dispersibility also in other biologically relevant media (e.g. NaCl 0.9% wt and PBS pH 7.4), exhibiting redox-responsiveness in the presence of gluthatione as reducing agent.

Introduction

Cancer is among the leading causes of premature mortality worldwide.[1] According to the World Health Organization, cancer currently accounts for approximately one in six deaths globally, although advances in surgical and chemotherapeutic interventions have significantly improved patient life expectancy and quality of life. In this context, nanotechnology-based drug delivery systems have emerged as a promising approach in cancer therapy, enabling sustained drug concentrations within the therapeutic window and, when required, site-specific delivery.[2] Nanocarriers can overcome key pharmacokinetic barriers by improving drug solubility, stability, bioavailability and circulation time. Furthermore, nanocarrier-mediated co-delivery of two or more therapeutic agents can enhance the overall efficacy of combination treatments.

It has been often considered polyphenols as strategic biochemical tools that can recalibrate a cancer cell's internal signalling [3] and sensitize tumor cells to chemo- and radiotherapy, by inhibiting pathways that lead to treatment resistance.[4] Curcumin (CUR) is a natural polyphenolic compound extracted from *Curcuma longa* L. and has long been used in traditional medical systems such as Ayurveda and Chinese medicine. Structurally, CUR is a symmetric seven-carbon molecule characterized by an α,β-unsaturated β-diketone moiety linking two *o*-methoxy phenolic groups.[5] Owing to the presence of the 1,6-heptadiene-3,5-dione chain, CUR undergoes keto–enol tautomerism, a feature that influences its interaction with nucleophiles as well as its hydrophobicity, polarity, and overall biomedical properties.[6] In general, the more stable enolic form predominates, enabling the formation of a strong intramolecular hydrogen bond that maintains the two oxygen atoms on the same side of the molecule and allows extended conjugation between the π-electron systems of the two feruloyl moieties. CUR is among the most extensively studied natural polyphenols due to its wide range of pharmacological activities,[7] including antioxidant, anti-inflammatory,[8] antibacterial,[9] and antiviral properties[10] and most notably its anticancer activity.[11] CUR has demonstrated efficacy against numerous cancer types,[12] including triple negative breast cancer, one of the most aggressive malignant neoplasms.[13] Despite these promising properties, phase I and II clinical trials across various disease models have revealed major limitations associated with CUR, primarily the requirement for high doses to achieve significant pharmacological effects. Curcumin shows a poor intestinal permeability, it is rapidly metabolized in the liver and predominantly eliminated via faeces. Its low bioavailability – attributable to poor aqueous solubility, low serum concentrations, limited tissue distribution, and extensive conjugation – has led to its classification within the Pan-Assay Interference Structures (PAINS) family.[14] Nevertheless, research on curcumin remains highly active, particularly in oncology, where it has shown notable anti-metastatic effects, especially when administered in combination with other anticancer agents.

Over the years, nanotechnology has emerged as a promising solution to bypass the critical delivery issues of CUR and enhance its multivalent biological, chemical and photochemical properties. Extensive research has been directed towards various carrier system[15] from liposomes,[16] micelles,[17, 18] hybrid nanoparticles, [19, 20] metal-organic framework,[21] exosomes,[22] biopolymers based-nanosystems [23] and nanocomposites. [24] However, several unresolved issues – including particle size variability, agglomeration, non-uniform size distribution, non-specific cellular uptake, and poorly controlled drug release – continue to compromise therapeutic efficacy and may induce adverse effects such as organ toxicity and immune responses.[25] These limitations underscore that the controlled and safe delivery of CUR remains an open challenge, particularly in cancer therapy, where prolonging patient survival while minimizing toxicity to healthy tissues has yet to be fully achieved.

[a] Dept. of Chemical, Biological, Pharmaceutical and Environmental Sciences (ChiBioFarAm), University of Messina, Viale F. Stagno d'Alcontres, 31, 98166 Messina, Italy.
[b] National Research Council, Institute for Nanostructured Materials (CNR-ISMN) URT of Messina at Dept. of Chemical, Biological, Pharmaceutical and Environmental Sciences (ChiBioFarAm), University of Messina, Viale F. Stagno d'Alcontres, 31, 98166 Messina, Italy.

Cyclodextrins (CDs) are among the most extensively investigated carriers for CUR due to their favourable chemical architecture and established pharmaceutical relevance. By forming host–guest supramolecular complexes with defined stoichiometry, CDs can enhance the aqueous solubility and stability of CUR and facilitate its delivery across cell membranes and towards biomolecular targets, thereby reducing cytotoxicity at appropriate doses.[26, 27] Nevertheless, conventional CD-based systems exhibit several intrinsic drawbacks that limit their translational potential. Low complexation efficiency can significantly reduce the effective drug payload, necessitating higher carrier-to-drug ratios that may introduce safety concerns. Moreover, reports of haemolysis and nephrotoxicity associated with certain CD formulations raise critical issues regarding their systemic administration. To address these shortcomings, CD functional nanoscale drug delivery platforms[28] have been developed, including linear polymerized β-cyclodextrins, crosslinked architectures such as β-cyclodextrin nanosponges,[29] stimuli responsive CD materials for CUR controlled release,[30] supramolecular CD polymers-based nanotubes,[31] and amphiphilic cyclodextrin (aCD) derivatives.[32] While these systems have demonstrated improved CUR loading and bioavailability, challenges related to reproducibility, batch-to-batch variability, scalability, and precise control over drug release kinetics persist. Consequently, the design of CD-based delivery nanoplatforms that combine high CUR complexation efficiency, predictable release behavior, and an acceptable safety profile remains a challenge,[33] warranting continuous investigations.

In the framework of our ongoing research of aCD nanoassemblies entrapping anticancer drugs,[34] photo-therapeutics and adamantane (ADA) conjugates with receptor targeting groups,[35] here we newly explore the incorporation of an ADA covalently conjugate with a therapeutic agent within aCD. ADA – a highly symmetric polycyclic cage structure – is known to form stable inclusion complexes with β-CDs due to its size compatibility with the CD cavity. The adamantyl fragment has proven to be a versatile structural element in medicinal chemistry, often acting as a lipophilic anchor capable of improving the pharmacokinetic behavior of drug-like molecules,[36] membrane permeability, metabolic stability and target binding of bioactive compounds.[37] Despite the extensive use of adamantane as a lipophilic scaffold in medicinal chemistry and the large number of derivatives of curcumin developed to improve its pharmacological properties, covalent conjugates combining these two structural motifs remain surprisingly underexplored in the literature.[38-41] Specifically, the aim of this work is to describe the synthesis of a novel curcumin derivative (**CUR-S-S-ADA**) and its supramolecular assembly with the aCD **SC6OH**[35] to afford the system **CUR-S-S-ADA@SC6OH**. This complex was characterized by complementary spectroscopic techniques (UV/Vis, steady-state fluorescence emission and DLS) to elucidate their physicochemical properties and the ability to enhance CUR solubility in biologically relevant media. In **CUR-S-S-ADA**, CUR is covalently linked to ADA through a disulfide bond. The incorporation of a disulfide moiety was designed to confer in principle redox sensitivity to the conjugate, potentially enabling intracellular enzymatic reduction and subsequent release of CUR under biologically relevant redox conditions.

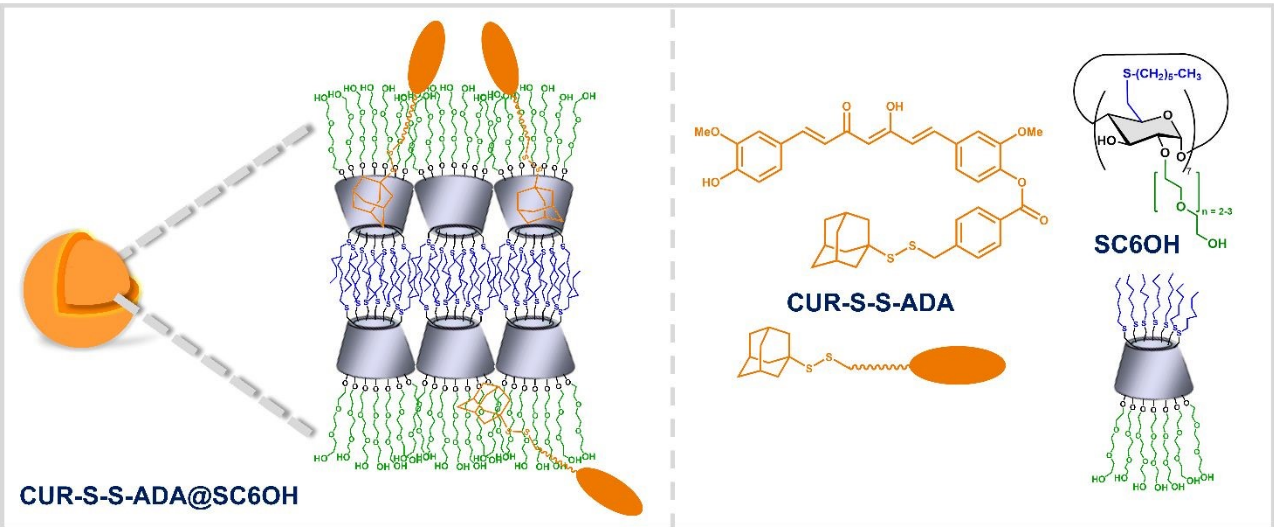

Chart 1. Schematization of the nanoassemblies components

Results and discussion

Synthetic procedures and properties

Synthesis of CUR-S-S-ADA. The synthetic strategy devised for the preparation of the unsymmetrical disulfide **CUR-S-S-ADA** (Scheme 1) involves the thermolysis of a suitable sulfenic acid precursor to generate *in situ* the corresponding sulfenic acid[42] that condenses with commercially available 1-adamantanethiol. This approach follows a well-established protocol[43] and proceeds under neutral conditions, thereby avoiding acidic or basic media that could compromise the integrity of the native CUR scaffold.[44]

View Article Online
DOI: 10.1039/D6OB00537C

ARTICLE

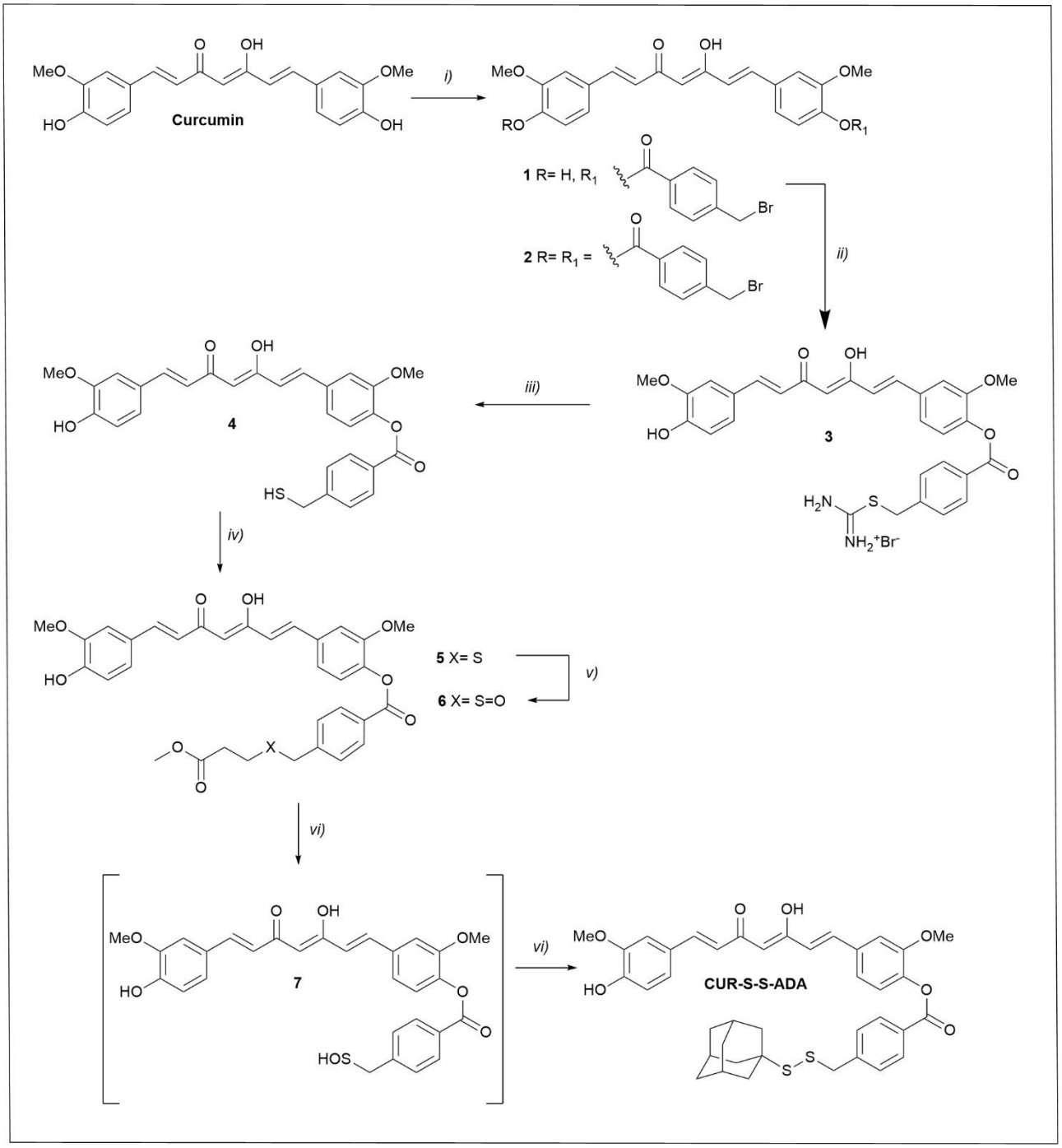

Scheme 1. Synthetic steps to **CUR-S-S-ADA**: *i)* 4-(bromomethyl) benzoic acid, DMAP, DCC, CH_2Cl_2, rt, 48 h; *ii)* thiourea, $CHCl_3$/EtOH, 50°C, 24 h; *iii)* $Na_2S_2O_5$, DCM/H_2O 1:2, reflux, 6 h; *iv)* methyl acrylate, TRITON B, THF, -78°C, 6 h; *v)* m-CPBA, DCM, -78°C, 5 min; *vi)* 1-adamantanethiol, 1,2-DCE, 83°C.

CUR was reacted at room temperature with 4-(bromomethyl)benzoic acid in the presence of N,N'-dicyclohexylcarbodiimide (DCC) and a catalytic amount of 4-dimethylaminopyridine (DMAP). Purification of the crude mixture by

View Article Online
DOI: 10.1039/D6OB00537C

column chromatography afforded the monobrominated derivative **1** and the curcumin bis-bromide **2** in 43% and 35% yield, respectively (Scheme 1). Reaction of compound **1** with thiourea at 50°C for 24 h gave the corresponding thiouronium salt **3** that was subsequently reduced with sodium metabisulfite (Scheme 1). After purification, CUR monothiol **4** was obtained in 58% yield.

The condensation of a suitable sulfenic acid with a thiol requires the preparation of an appropriately substituted sulfinyl precursor[45] identified as compound **6** (Scheme 1). Sulfoxide **6** was found to be readily handled, sufficiently stable under standard conditions, and suitably reactive upon thermolysis at temperatures above 80°C.[46] For the nucleophilic addition of thiol **4** to methyl acrylate, benzyl trimethylammonium hydroxide (Triton B) was employed as a base in catalytic amounts at −78°C, affording sulfide **5** in 60% yield (Scheme 1). Subsequent oxidation of sulfide **5** with *m*-chloroperbenzoic acid (*m*-CPBA) at −78°C furnished sulfoxide **6**, which was separated from trace amounts of the corresponding sulfone by column chromatography and isolated in 80% yield. Thermolysis of CUR derivative **6** with 1-adamantanethiol was performed in 1,2-dichloroethane (1,2-DCE) under reflux for 6 h. Purification by column chromatography afforded **CUR-S-S-ADA** in 50% yield.

The cytotoxic effect of compound **CUR-S-S-ADA** was investigated using a mitochondrial cytotoxicity assay. Specifically, murine fibroblast NIH-3T3 cell viability was assessed by means of the thiazolyl blue tetrazolium bromide (MTT) assay, which reflects cellular metabolic activity. As shown in SI (Figure S11), when evaluated at the concentration tested as compatible with curcumin cellular models, **CUR-S-S-ADA** showed no cytotoxic effects.[47]

Preparation of CUR–S-S–ADA@SC6OH nanoassemblies. **CUR–S–S–ADA** was mixed with an excess of **SC6OH** in a dichloromethane (DCM) solution.[35] The mixture was stirred and subsequently evaporated to afford an organic film of the **CUR–S–S–ADA@SC6OH** complex. The resulting film was then hydrated with water or physiological saline solution (NaCl 0.9% wt) or in PBS buffer (pH 7.4) and subjected to sonication, leading to the formation of **CUR–S–S–ADA@SC6OH** nanoassemblies in aqueous solution (Scheme 2). The optimized procedure to obtain **CUR-S-S-ADA@SC6OH** nanoassemblies relies on the solvent-evaporation method previously reported for similar systems.[32] Nanoassemblies were prepared at 1:2 molar ratio keeping the **CUR-S-S-ADA** nominal concentration at 20 µM. The 1:2 formulation was selected as optimal compromise, providing satisfactory **CUR-S-S-ADA** loading while minimizing the excess of amphiphilic cyclodextrin. This ratio corresponds to one of the most commonly reported stoichiometries for complexes between CUR and pristine or functionalized cyclodextrins, with 1:2 systems being structurally relevant and often associated with improved encapsulation efficiency and solubility.[26, 48] Moreover, it allows direct comparison with the system previously reported by our group.[32]

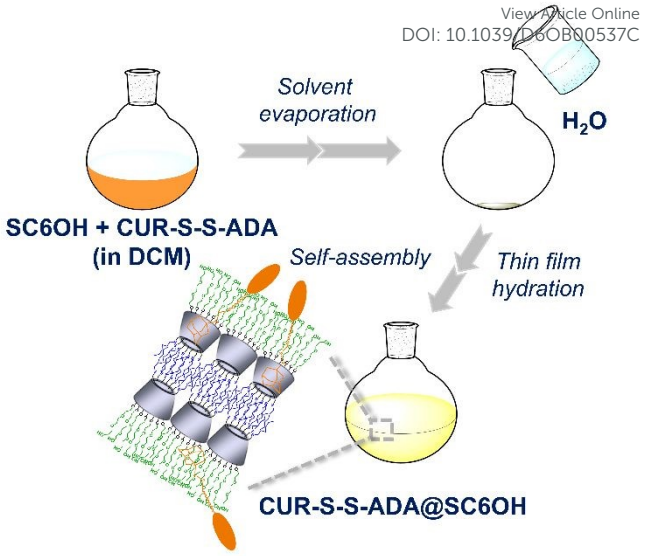

Scheme 2. Preparation scheme of **CUR-S-S-ADA@SC6OH** nanoassemblies

Characterization of the nanoassemblies

The photophysical properties of **CUR-S-S-ADA** were first investigated in DCM by UV/Vis absorption and steady-state fluorescence spectroscopies. As shown in Figure 1a, the absorption spectrum displays a prominent band centred at 410 nm, which can be attributed to a π-π* transition associated with the conjugated curcuminoid scaffold, and a shoulder at 434 nm.

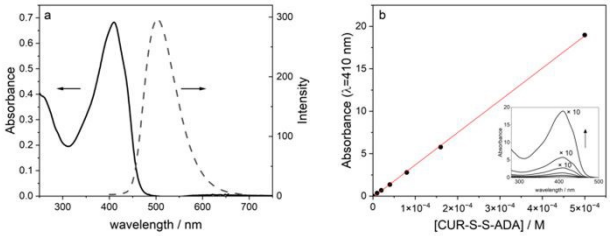

Figure 1. (a) UV/Vis absorption and emission spectra of **CUR-S-S-ADA** in DCM. [CUR-S-S-ADA] = 20 µM, λ_{exc} = 320 nm, path length 10 mm. (b) Calibration curve for **CUR-S-S-ADA** in DCM in the concentration range 10-500 µM. $\varepsilon_{410\ nm} = 3.8 \times 10^4 \pm 0.03\ M^{-1}\ cm^{-1}$, ($R^2$ = 0.999). In the inset the corresponding UV/Vis spectra. Path length 1-10 mm.

According to the literature,[49, 50] these spectral features are similar to those observed in other aprotic solvents and are due to the exclusive presence of the enolic form of CUR derivatives in the ground state. The molar extinction coefficient of **CUR-S-S-ADA** ($\varepsilon_{410nm} \approx 38039\ M^{-1}\ cm^{-1}$) in DCM was determined in the concentration range 10-500 µM (Figure 1b). Upon excitation, **CUR-S-S-ADA** exhibits a broad fluorescence emission band with a maximum around 510 nm (Figure 1a). The broad emission profile reflects structural and electronic relaxation occurring in the excited state.[51] A pronounced Stokes shift of approximately 100 nm is observed, indicating significant excited-state relaxation processes, consistent with the intramolecular charge-transfer (ICT) character commonly

View Article Online
DOI: 10.1039/D6OB00537C

observed in curcuminoid chromophores arising from the extended π-conjugated system.[6] UV/Vis absorption and steady-state fluorescence emission measurements were carried out to investigate the interaction between **CUR-S-S-ADA** and amphiphilic cyclodextrin nanoassemblies. Figure 2 shows the UV/Vis absorption spectra of **CUR-S-S-ADA** entrapped within **SC6OH** nanoassemblies together with that recorded in DCM for comparison.

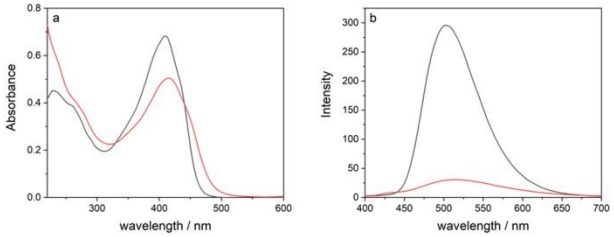

Figure 2. (a) UV/Vis absorption spectra of **CUR-S-S-ADA** (black line) in DCM and **CUR-S-S-ADA@SC6OH** (red line) at 1:2 molar ratio in ultrapure water and (b) the corresponding emission spectra. [CUR-S-S-ADA] = 20 μM, λ_{exc} = 320 nm.

The absorption spectrum of CUR-S-S-ADA entrapped inside SC6OH nanoassemblies exhibits a slight broadening and a red shift (*ca*. 8 nm) with respect to that recorded in DCM. Despite the aqueous medium the absorption profile still retains a partially resolved vibronic structure. This observation suggests that the chromophore is located in a relatively hydrophobic local microenvironment within the cyclodextrin assemblies, which partially preserves the spectral features observed in organic solvent, suggesting partial shielding of the chromophore from the aqueous environment. The fluorescence emission spectrum of the CUR derivative recorded in DCM exhibits an intense and broad band with a maximum centred at 503 nm. Consistently with the absorption behaviour, the emission band becomes slightly red-shifted and significantly broadened when CUR-S-S-ADA is loaded into SC6OH in aqueous solution. At the same time, a marked decrease in fluorescence intensity is observed, while the overall spectral profile remains relatively similar. The pronounced fluorescence quenching suggests the occurrence of increased non-radiative deactivation pathways, likely mediated by the solvent and from partial aggregation of the CUR derivative within the cyclodextrin nanoassemblies. A similar spectroscopic scenario is commonly observed for curcumin derivatives in polar environment, where hydrogen-bonding interactions and changes in tautomeric equilibrium can promote nonradiative decays.[49]

The colloidal behaviour of the nanoassemblies was further investigated by dynamic light scattering (DLS) measurements on aqueous dispersions of SC6OH and CUR-S-S-ADA@SC6OH. In ultrapure water, SC6OH forms two populations of nanoassemblies with mean hydrodynamic diameters (D_H) of *ca*. 20 nm and 260 nm and a ζ-potential value of about -34 mV, indicating the formation of negatively charged colloidally stable aggregates. Upon loading of CUR-S-S-ADA, the bimodal size distribution is preserved, although slight changes in the aggregate dimensions are observed. As shown in Figure 3, the CUR-S-S-ADA@SC6OH exhibits two families of aggregates with hydrodynamic diameters of *ca*. 30 nm and 220 nm.

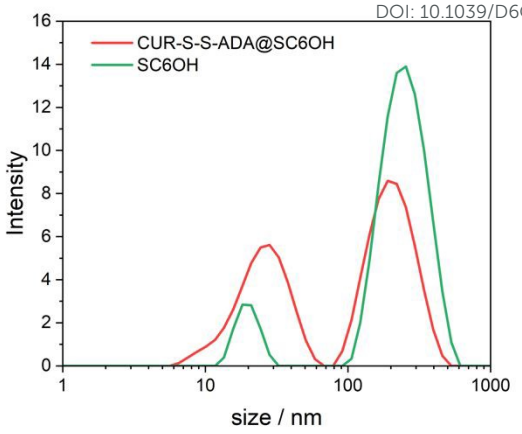

Figure 3. Size distribution of **SC6OH** (green line) and **CUR-S-S-ADA@SC6OH** (red line) at 2:1 molar ratio in ultrapure water. [CUR-S-S-ADA] = 20 μM, T = 25°C.

Compared to the unloaded **SC6OH** assemblies, the smaller population displays an increase in size whereas the larger slightly decreases in size. In addition to the change in size, the relative abundance of the two populations is significantly altered, shifting from about 10:90 ratio in unloaded **SC6OH** assemblies to approximately 50:50 ratio after **CUR-S-S-ADA** loading. This redistribution likely reflects a perturbation of the self-assembly equilibrium of **SC6OH** induced by **CUR-S-S-ADA** loading, resulting in a partial rearrangement and/or disassembling of the nanoaggregate structure. Consistently, a variation in the ζ-potential is observed upon loading of CUR-S-S-ADA, shifting from −34 mV for the unloaded SC6OH assemblies to −12 mV for the CUR-S-S-ADA@SC6OH system. The decrease in the absolute value of the surface charge suggests partial screening of the surface charges and a concomitant rearrangement of the nanoassembly organization upon **CUR-S-S-ADA** incorporation.

The system was scaled up by increasing the overall concentration ten-fold maintaining the same stoichiometric ratio in order to evaluate whether the robustness of the nanoassembly formation was preserved under conditions more relevant for drug delivery. Notably, **SC6OH** nanoassembly allowed the dissolution of **CUR-S-S-ADA** up to 0.14 mg/mL under these conditions, a concentration significantly higher compared to the solubility of free curcumin in pure water at room temperature (approximately 0.6 μg/mL). The size and ζ-potential values for **CUR-S-S-ADA@SC6OH** are summarized in Table 1.

Table 1. Mean hydrodynamic diameter (D_H) and ζ-potential values for **CUR-S-S-ADA@SC6OH** from DLS analysis.

	D_H / nm (A%)	PDI	ζ / mV
SC6OH	260 ± 88 (89) 20 ± 3 (11)	0.11 0.02	-34 ± 5
CUR-S-S-ADA@SC6OH[a]	217 ± 91 (54) 28 ± 13 (46)	0.18 0.22	-12 ± 5
CUR-S-S-ADA@SC6OH[b]	268 ± 118 (48) 24 ± 11 (52)	0.19 0.21	-11 ± 5
CUR-S-S-ADA@SC6OH[c]	269 ± 100	0.14	-

[CUR-S-S-ADA] = 20 μM[a], 200 μM[b]. [c]NaCl (0.9% wt)

View Article Online
DOI: 10.1039/D6OB00537C

Colloidal stability

CUR-S-S-ADA@SC6OH was dispersed in NaCl 0.9% wt and in PBS buffer, as medium commonly used in biological and preclinical studies. Under these conditions the nanoassemblies remained well dispersed. The stability of **CUR–S–S–ADA@SC6OH** was monitored over 24 h in PBS (10 mM, pH 7.4, T = 25°C and the results are reported in Figure S12. Nanoassemblies were fairly stable in PBS mimicking the physiological conditions, as demonstrated by the slight reduction of the absorbance maximum. It well-known that CUR can be stabilized by storage as CUR/β-CD nanoparticles [52] or by previous complexation with (2-hydroxypropyl)-β-cyclodextrin (HP-β-CD) and following encapsulation in polymeric nanoparticles[53]. Similarly to these reports where CD plays a key role in the stabilization of CUR, CUR encapsulated in SC6OH is stable in biologically relevant media for about 3 days.[32] Furthermore, the CUR conjugate CUR-S-S-Ada was designed to be stimuli-responsiveness accelerating the detachment of CUR upon GSH action. Therefore, its stability in PBS over 24 h can be in perspective exploited for redox-responsive cell-uptake.

However, particular attention was focused to the redox-responsive disulfide linker connecting the curcumin scaffold to the adamantane moiety, which acts as a cyclodextrin-targeting moiety. The disulfide bond can be cleaved by glutathione (GSH), thus triggering the release of the drug. Preliminary experiments were carried out to evaluate the responsiveness of the system under reductive conditions. The nanoassemblies were incubated with GSH and the resulting spectroscopic changes were monitored over time. As shown in Figure 4, the addition of GSH induces significant changes in both absorption and emission profiles. The increase in fluorescence intensity observed after 24 h of incubation suggests that reductive cleavage of the disulfide linkage alters the local environment of **CUR-S-S-ADA**. Such behaviour is consistent with a rearrangement of the reduced species (presumably **4**) within the nanoassemblies, leading to a less quenched environment rather than its complete release into the PBS solution. Additionally, the slight blue shift observed in the absorption spectrum after GSH addition further supports the location of the curcuminoid chromophore in a less polar microenvironment after reductive cleavage of the disulfide bridge. Nevertheless, a possible contribution from an increased fluorescence quantum yield of the reduced species relative to **CUR-S-S-ADA** cannot be excluded.

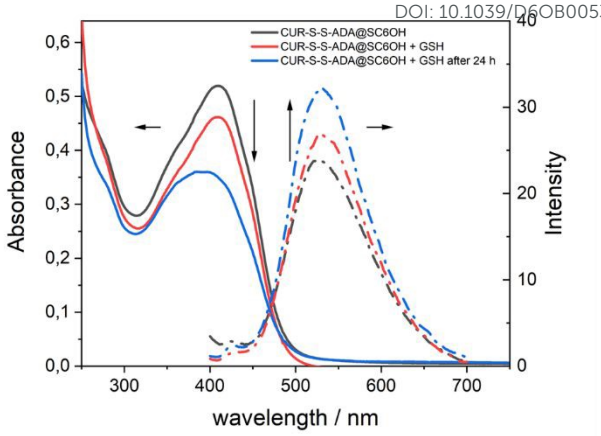

Figure 4. UV/Vis and emission spectra of **CUR-S-S-ADA@SC6OH** in PBS buffer (pH 7.4) in the presence of glutathione (GSH). [CUR-S-S-ADA] = 20 μM, [GSH] = 15 mM, T = 25°C.

Experimental

General information

Curcumin from *Curcuma longa* (C1386, purity 65%, Sigma-Aldrich) was purified by column chromatography on silica gel using $CHCl_3$/*n*-hexane 9:1 as the eluent; other commercial reagents and solvents were used without further purification. Heptakis(2-O-(oligoethyleneglycol)-6-hexylthio)-βCD, (SC6OH), with an average of 24 units of ethylene oxide (EO) and the most abundant peak at about 2935 Da, was synthesized according to the general procedure.[32] The syntheses of compounds **1**-**6** were reported in the Supporting Information (SI). The reactions were monitored by TLC (precoated aluminium plates of silica gel 60 F_{254}) and the products were visualized with vanillin [1 g dissolved in MeOH (60 mL) and conc. H_2SO_4 (0.6 mL)] and/or by a UV lamp. Column chromatography was performed using Silica gel 60. ^{1}H and ^{13}C NMR spectra were recorded in $CDCl_3$ with a Varian 500 spectrometer (at 500 MHz for ^{1}H and 125 MHz for ^{13}C). Chemical shifts are given in parts per million (ppm) referenced to the residual protons in $CDCl_3$ (δ 7.26 ppm for ^{1}H NMR and δ 77.16 ppm for ^{13}C NMR) solvents. NMR peak assignments are supported by homonuclear (COSY, correlation spectroscopy) and heteronuclear correlation ^{1}H–^{13}C spectroscopy (HSQCAD). Coupling constants (J) are given in Hertz. Numbering of atoms of curcumin-based compounds is reported in the spectra shown in SI. Melting points were determined using Kofler hot-stage apparatus and are uncorrected. Combustion analyses were carried out on a FISONS EA1108 elemental analyser.

Synthetic procedures

Synthesis of compound CUR-S-S-ADA. To a solution of compound **6** (55 mg, 0.088mmol, 1 eq.) in 1,2-dichloroethane (6 mL) 1-adamantanethiol (45 mg, 0.264 mmol, 3 eq.) was added. The mixture was stirred under inert atmosphere at reflux for 12 h, until the disappearance of **6** (TLC n-hexane/Ethyl Acetate 5:5). The solvent was removed under reduced pressure, and the crude was purified by

View Article Online
DOI: 10.1039/D6OB00537C

column chromatography (SiO_2, *n*-hexane/Ethyl Acetate 7:3 to 5:5) to give **CUR-S-S-ADA** as yellow solid (yield 34%). M.p.: 154–158 °C. R_f: 0.7 (*n*-hexane/Ethyl Acetate 5:5). ^{1}H NMR ($CDCl_3$, 500 MHz): δ 8.17 and 7.45 (2x d, 4H, *J*= 8.2 Hz) [H-13 and H-14]; 7.64, 7.62, 6.58 and 6.50 (4x d, 4H, *J*= 16.0 Hz) [H-3, H-4, H-3' and H-4']; 7.22-7.16 (m, 3H) [H-6; H-9 and H-10]; 7.13 (dd, 1H, *J*= 8.2 Hz, *J*= 2.0 Hz) [H-10']; 7.06 (d, 1H, *J*= 2.0 Hz) [H-6']; 6.94 (d, 1H, *J*= 8.2 Hz) [H-9']; 5.88 (s, 1H) [-OH]; 5.84 (s, 1H) [H-1]; 3.95 and 3.86 (2x s, 6H) [2x -OMe]; 3.94 (s, 2H) [H-16]; 2.13-2.06 (m, 3H) [H-γ]; 1.88 (d, 6H, *J*= 3.0 Hz) [H-β]; 1.74-1.66 (m, 6H) [H-δ]. ^{13}C NMR ($CDCl_3$, 125 MHz): δ 184.6 and 182.0 [C-2 and C-2']; 164.4 [C-11]; 151.8, 148.1, 147.0, 143.9 and 141.6 [Cq]; 141.2, 139.6, 124.4 and 121.9 [C-3, C-4, C-3' and C-4']; 134.3, 128.2 and 127.7 [Cq]; 130.7 and 129.6 [C-12 and C-13]; 123.6, 121.2 and 111.7 [C-6, C-9 and C-10]; 123.2 [C-6']; 115.0 [C-9']; 109.8 [C-10']; 101.1 [C-1]; 56.1 [-OMe]; 50.1 [C-16]; 45.7 [C-α]; 42.8 [C-β]; 36.2 [C-δ] and 30.0 [C-γ]. Anal. calcd for $C_{39}H_{40}O_7S_2$: C, 68.40; H, 5.89; O, 16.35; S, 9.36. Found: C, 68.43; H, 5.92.

Preparation of CUR-S-S-ADA@SC6OH nanoassemblies. Nanoassemblies were prepared at 1:2 molar ratio, with **CUR-S-S-ADA@SC6OH** nominal concentration of 20 μM or 200 μM, according to previously reported procedures.[32] Briefly, an organic film was obtained by slow evaporation of a mixed solution of **SC6OH** and **CUR-S-S-ADA@SC6OH** in DCM at desired molar ratio. The resulting film was then hydrated with ultrapure water solution or in physiological saline solution (NaCl 0.9 % wt) or PBS buffer (pH 7.4) and sonicated in ultrasonic bath for about 20 min. Unloaded **CUR-S-S-ADA@SC6OH** was removed from the nanoassemblies by slight centrifugation of the dispersions (5000 rpm). The actual Drug Loading (*DL*), Theoretical Loading (*TL*) and Entrapment Efficiency (*EE*) were determined by Equations 1–3, respectively. *DL* determined by Equation (1), was 10.6 %, and was almost equal to *TL* Equation (2). The entrapment efficiency, calculated by Equation (3), was nearly 100 %.

$$(DL)\% = \frac{amount\ of\ CUR\text{–}S\text{–}S\text{–}ADA\ in\ nanoassembly}{weighted\ amount\ of\ nanoassembly} \times 100 \quad (1)$$

$$(TL)\% = \frac{amount\ of\ CUR\text{–}S\text{–}S\text{–}ADA\ initiallty\ added\ to\ formulation}{weighted\ amount\ of\ nanoassembly} \times 100 \quad (2)$$

$$(EE)\% = \frac{amount\ of\ CUR\text{–}S\text{–}S\text{–}ADA\ in\ nanoassembly}{amount\ of\ CUR\text{–}S\text{–}S\text{–}ADA\ initially\ added\ to\ formulation} \times 100 \quad (3)$$

Characterization methods

***Size and ζ-potential of nanoassemblies*.** The hydrodynamic diameter (D_H), width of distribution (poly dispersity index, PDI) of the empty **SC6OH** and **CUR-S-S-ADA@SC6OH** nanoassemblies, and ζ-potential were measured through dynamic light scattering (DLS) by a Zetasizer Nano ZS (Malvern Instrument, Malvern, U.K.) equipped with a He-Ne laser at a power of 4.0 mW and λ = 633 nm. The measurements were performed at a 173° angle with respect to the incident beam at 25 ±1°C for each dispersion of **SC6OH** and **CUR-S-S-ADA@SC6OH** using ultrapure water or NaCl (0.9 % wt) where specified as dispersing media. The deconvolution of the measured correlation curve to an intensity size distribution was obtained by using a non-negative least-squares algorithm. The results are expressed as the mean of three independent measurements performed on three different batches.

UV/Vis and steady-state fluorescence emission spectroscopies. UV/Vis absorption spectra were recorded on a Hewlett-Packard (Agilent) model 8453 diode array spectrophotometer using 0.1–1 cm path length quartz cell. Extinction coefficients of **CUR-S-S-ADA@SC6OH** in DCM (ε_{410}) was determined by Lambert and Beer law in the concentration range 10-500 μM. A UV/Vis neutral filter was placed on the observation path to avoid the photoproduction of hydrochloric acid at the interface between the light-exposed cuvette silica wall and the bulk solvent when DCM was used as dispersing media. Emission fluorescence spectra were recorded on a Jasco model FP-750 spectrofluorometer by using a 1 cm path length quartz cell using excitation wavelength of 320 nm.

Conclusions

Nanoassemblies based on a novel disulfide-linked adamantane–curcumin conjugate and a non-ionic amphiphilic cyclodextrin (CUR-S-S-ADA@SC6OH) were successfully designed and thoroughly characterized in aqueous dispersion. The resulting nanoassemblies exhibited high loading capacity for the curcumin derivative (up to 0.14 mg mL^{-1}) and excellent dispersibility in biologically relevant media (0.9 wt% NaCl and PBS at pH 7.4). Noteworthy, preliminary spectroscopic evidence indicates that these systems are redox-responsive, as the disulfide linkage can be cleaved by glutathione (GSH), thereby triggering curcumin release. These findings highlight the potential of this supramolecular platform for the development of redox-responsive nanotherapeutics for controlled drug delivery.

Author contributions

Roberto Zagami: Data Curation, Formal Analysis, Investigation, Methodology, Visualization, Writing – Original Draft. **Chiara M.A. Gangemi**: Data Curation, Formal Analysis, Investigation, Methodology, Writing – review & editing. **Giuseppe Nocito**: Visualization, Writing – review & editing. **Alberto Aricò**: Investigation, Methodology. **Maura Monforte:** Investigation Methodology. **Paola M. Bonaccorsi**: Conceptualization, Funding acquisition, Methodology, Project administration, Supervision, Writing – Original Draft, Writing – review & editing. **Antonino Mazzaglia**: Conceptualization, Funding acquisition, Methodology, Project administration, Supervision, Writing – review & editing.

Conflicts of interest

In accordance with our policy on Conflicts of interest please ensure that a conflicts of interest statement is included in your manuscript here. Please note that this statement is required for all submitted manuscripts. If no conflicts exist, please state that "There are no conflicts to declare".

Acknowledgements

We are grateful to Dr. Milo Malanga (Carbohyde, Budapest) for providing amphiphilic cyclodextrin. We are also grateful to Prof. Davide Barreca (Dept. ChiBioFarAm, University of Messina) for cytotoxicity studies. This work was supported by the European Union (NextGenerationEU) through the Italian Ministero dell'Università e della Ricerca (MUR) Piano Nazionale Ripresa e Resilienza (PNRR) project SAMOTHRACE "SiciliAn MicrOnanoTecH Research And innovation CEnter" ECS: 00000022 – CUP: B63C22000620005.

Notes and references

1 C. Frick, H. Rumgay, J. Vignat, O. Ginsburg, E. Nolte, F. Bray and I. Soerjomataram, *The Lancet Global Health*, 2023, **11**, e1700-e1712.
2 Y. Xue, Y. Gao, F. Meng and L. Luo, *Cancer Biology and Medicine*, 2021, **18**, 336.
3 S. Fakhri, S. Z. Moradi, S. Y. Moradi, S. Piri, B. Shiri Varnamkhasti, S. Piri, M. R. Khirehgesh, A. Bishayee, N. Casarcia and A. Bishayee, *BMC Cancer*, 2024, **24**, 1079.
4 S. Fakhri, S. Z. Moradi, F. Faraji, T. Farhadi, O. Hesami, A. Iranpanah, K. Webber and A. Bishayee, *Cancer and Metastasis Reviews*, 2023, **42**, 959-1020.
5 C. M. Gangemi, S. Mirabile, M. Monforte, A. Barattucci and P. M. Bonaccorsi, *International Journal of Molecular Sciences*, 2025, **26**(10), 4871.
6 M. Ghosh and N. Sarkar, *ChemBioChem*, 2024, **25**, e202400335.
7 S. Bhattacharya, *Pharmacological Research - Natural Products*, 2026, **10**, 100541.
8 H. Sowmya Lakshmi, S. Subhashini, D. Rajkumar and R. Ramesh, in *Recent Advances in Oxidative Stress Associated Chronic Diseases Volume 2: A Review of The Health Benefits and Risks of The Substance*, eds. K. Kasinathan and A. Muthukumaran, Springer Nature Singapore, Singapore, 2026, https://doi.org/10.1007/978-981-95-3758-7_2, pp. 15-51.
9 N. Burduja, N. F. Virzì, G. Nocito, G. Ginestra, M. G. Saita, F. Spitaleri, S. Patanè, A. Nostro, V. Pittalà and A. Mazzaglia, *International Journal of Pharmaceutics*, 2025, **672**, 125283.
10 A. Ardebili, M. H. Pouriayevali, S. Aleshikh, M. Zahani, M. Ajorloo, A. Izanloo, A. Siyadatpanah, H. Razavi Nikoo, P. Wilairatana and H. D. Coutinho, *Molecules*, 2021, **26**(22), 6994.
11 F. C. Rodrigues, N. V. Anil Kumar and G. Thakur, *European Journal of Medicinal Chemistry*, 2019, **177**, 76-104.
12 G. Kah, R. Chandran and H. Abrahamse, *Pharmaceutics*, 2023, **15**(2), 639.
13 P. M. Bonaccorsi, M. Labbozzetta, A. Barattucci, T. M. Salerno, P. Poma and M. Notarbartolo, *Pharmaceuticals*, 2019, **12**(4), 161.
14 E. Burgos-Morón, J. M. Calderón-Montaño, J. Salvador, A. Robles and M. López-Lázaro, *International Journal of Cancer*, 2010, **126**, 1771-1775.
15 Y.-S. Fu, T.-H. Chen, L. Weng, L. Huang, D. Lai and C.-F. Weng, *Biomedicine & Pharmacotherapy*, 2021, **141**, 111888.
16 V. V. Sokolik, O. H. Berchenko, N. O. Levicheva, Y. H. Kot, K. V. Kot, O. O. Tigunova, Y. B. Blume and S. M. Shulga, *Cytology and Genetics*, 2026, 60, 48-58.
17 L. Youssouf, A. Bhaw-Luximon, N. Diotel, A. Catan, P. Giraud, F. Gimié, D. Koshel, S. Casale, S. Bénard, V. Meneyrol, L. Lallemand, O. Meilhac, C. Lefebvre D'Hellencourt, D. Jhurry and J. Couprie, *Carbohydrate Polymers*, 2019, **217**, 35-45.
18 N. F. Virzì, A. N. Fallica, G. Romeo, K. Greish, M. A. Alghamdi, S. Patanè, A. Mazzaglia, M. Shahid and V. Pittalà, *RSC Advances*, 2023, **13**, 31059-31066.
19 A. Mahmoudi, P. Kesharwani, M. Majeed, Y. Teng and A. Sahebkar, *Colloids and Surfaces B: Biointerfaces*, 2022, **215**, 112481.
20 S. Riela, A. Barattucci, D. Barreca, S. Campagna, G. Cavallaro, G. Lazzara, M. Massaro, G. Pizzolanti, T. M. G. Salerno, P. Bonaccorsi and F. Puntoriero, *Dyes and Pigments*, 2021, **187**, 109094.
21 Y. Chen, J. Su, W. Dong, D. Xu, L. Cheng, L. Mao, Y. Gao and F. Yuan, *Food Chemistry*, 2022, **383**, 132605.
22 K. Pande, B. B K and A. Kannan, *Cancer Treatment and Research Communications*, 2026, **46**, 101102.
23 S. Chauhan, J. Naik, B. Patel and M. Patel, in *Functional Biochemistry of Micronutrients*, eds. N. S. Dhalla, P. S. Tappia and V. Elimban, Springer Nature Switzerland, Cham, 2026, https://doi.org/10.1007/978-3-032-14441-6_8, pp. 171-207.
24 M. S. A. Aziz, G. A.-E. Mahmoud, H. S. Abdel-Tawab, E. F. Abo Zeid and M. A. El-Aal, *Journal of Water Process Engineering*, 2026, **83**, 109586.
25 S. Jacob, F. S. Kather, M. A. Morsy, S. H. S. Boddu, M. Attimarad, J. Sah, P. Shinu and A. B. Nair, Nanomaterials, 2024, **14**(8), 672.
26 W. A. Alghamdi, S. S. Alterary, A. Alarifi, R. Ramu, M. S. Khan and M. Afzal, *International Journal of Biological Macromolecules*, 2024, **282**, 137238.
27 J. Li, F. Xu, Y. Dai, J. Zhang, Y. Shi, D. Lai, N. Sriboonvorakul and J. Hu, *Polymers*, 2022, **14**(24), 5421.
28 F. Topuz and T. Uyar, *WIREs Nanomedicine and Nanobiotechnology*, 2024, **16**, e1995.
29 Z. Husain, P. Nayak, S. Pandey, R. Paliwal and S. R. Paliwal, *Journal of Molecular Liquids*, 2026, **446**, 129289.
30 R. Sedghi, M. Yassari and B. Heidari, *Colloids and Surfaces B: Biointerfaces*, 2018, **162**, 154-162.
31 D. Zhang, Y. Liu, Y. Fan, C. Yu, Y. Zheng, H. Jin, L. Fu, Y. Zhou and D. Yan, *Advanced Functional Materials*, 2016, **26**, 7652-7661.
32 R. Zagami, A. Barattucci, L. Monsù Scolaro, M. Viale, G. Raffaini, P. Maria Bonaccorsi and A. Mazzaglia, *Journal of Molecular Liquids*, 2023, **389**, 122841.
33 H. M. Abdel-Mageed, N. Z. AbuelEzz, A. A. Ali, A. E. Abdelaziz, D. Nada, S. M. Abdelraouf, S. A. Fouad, A. Bishr and R. A. Radwan, *BMC Biotechnology*, 2025, **25**, 49.
34 M. L. Bondì, A. Scala, G. Sortino, E. Amore, C. Botto, A. Azzolina, D. Balasus, M. Cervello and A. Mazzaglia, *Biomacromolecules*, 2015, **16**, 3784-3791.
35 R. Zagami, V. Rapozzi, A. Piperno, A. Scala, C. Triolo, M. Trapani, L. E. Xodo, L. Monsù Scolaro and A. Mazzaglia, *Biomacromolecules*, 2019, **20**, 2530-2544.
36 I. González-Méndez, J. D. Solano, P. Porcu, A. Ruiu, Y. Rojas-Aguirre and E. Rivera, *Journal of Molecular Structure*, 2019, **1177**, 143-151.
37 L. Wanka, K. Iqbal and P. R. Schreiner, *Chemical Reviews*, 2013, **113**, 3516-3604.
38 R. Abonia, K. K. Laali, D. Raja Somu, S. D. Bunge and E. C. Wang, *ChemMedChem*, 2020, **15**, 354-362.
39 R. I. Al-Wabli, O. M. AboulWafa and K. M. Youssef, *Medicinal Chemistry Research*, 2012, **21**, 874-890.
40 Y. González, R. Mojica-Flores, D. Moreno-Labrador, M. Pecchio, K. S. J. Rao, M. Ahumedo-Monterrosa, P. L. Fernández, O. V. Larionov and J. Lakey-Beitia, *Molecules*, 2023, **28**(23), 7787.
41 D. V. T. Patel, Divya M.; Kanhed, Ashish M.; Patel, Nirav M.; Shah, Bhavik S.; Vora, Amisha K.; Chhabria, Mahesh T.; Yadav, Mange Ram, *International Journal of Quantitative Structure-Property Relationships*, 2021, **6**, 58-77.
42 M. C. Aversa, A. Barattucci, P. Bonaccorsi, C. Faggi and T. Papalia, *The Journal of Organic Chemistry*, 2007, **72**, 4486-4496.
43 C. M. A. Gangemi, E. D'Agostino, M. C. Aversa, A. Barattucci and P. M. Bonaccorsi, *Tetrahedron*, 2023, **143**, 133550.
44 M. C. Aversa, A. Barattucci and P. Bonaccorsi, *European Journal of Organic Chemistry*, 2009, 6355-6359.

View Article Online
DOI: 10.1039/D6OB00537C

45 M. C. Aversa, A. Barattucci, P. Bonaccorsi and A. Temperini, *European Journal of Organic Chemistry*, 2011, 5668-5673.
46 P. Bonaccorsi, F. Marino-Merlo, A. Barattucci, G. Battaglia, E. Papaianni, T. Papalia, M. C. Aversa and A. Mastino, *Bioorganic & Medicinal Chemistry*, 2012, **20**, 3186-3195.
47 L. M. Mendonça, G. C. dos Santos, G. A. Antonucci, A. C. dos Santos, M. d. L. P. Bianchi and L. M. G. Antunes, *Mutation Research/Genetic Toxicology and Environmental Mutagenesis*, 2009, **675**, 29-34.
48 P. Arya and N. Raghav, *Journal of Molecular Structure*, 2021, **1228**, 129774.
49 F. Laneri, C. Conte, C. Parisi, O. Catanzano, A. Fraix, F. Quaglia and S. Sortino, *Journal of Photochemistry and Photobiology B: Biology*, 2023, **245**, 112756.
50 M. H. M. Leung, M. A. Addicoat, S. F. Lincoln, G. F. Metha and T. W. Kee, *Physical Chemistry Chemical Physics*, 2024, **26**, 14970-14979.
51 C. F. Chignell, P. Bilskj, K. J. Reszka, A. G. Motten, R. H. Sik and T. A. Dahl, *Photochemistry and Photobiology*, 1994, **59**, 295-302.
52 L. Jiang, N. Xia, F. Wang, C. Xie, R. Ye, H. Tang, H. Zhang and Y. Liu, *LWT – Food Science and Technology*, 2022, **171**, 114149.
53 C. Serri, M. Argirò, L. Piras, D. G. Mita, A. Saija, L. Mita, M. Forte, S. Giarra, M. Biondi, S. Crispi and L. Mayol, *International Journal of Pharmaceutics*, 2017, **520**, 21-28.

View Article Online
DOI: 10.1039/D6OB00537C

Data availability statements

The data supporting this article have been included as part of the Supplementary Information.